Compensated interferometry measures of CYFRA 21-1 improve diagnosis of lung cancer

Authors: Michael N. Kammer[1], Amanda K. Kussrow[1], Rebekah L. Webster[1], Heidi Chen[2], Megan Hoeksema[3], Robert Christenson[4], Pierre P. Massion[3], and Darryl J. Bornhop[1]*

Affiliations:

[1]Department of Chemistry and The Vanderbilt Institute for Chemical Biology, Vanderbilt University, Nashville, TN, 37235

[2]Department of Biostatistics, Vanderbilt University Medical Center, Nashville, TN, 37232

[3]Division of Allergy, Pulmonary and Critical Care Medicine and Vanderbilt-Ingram Cancer Center, Vanderbilt University Medical Center, Nashville, TN, 37232.

[4]Department of Pathology, University of Maryland, Baltimore, MD, 21201

*To whom correspondence should be addressed: Darryl.bornhop@vanderbilt.edu

One Sentence Summary: A novel label-free biomarker assay and interferometric reader are shown to provide improved performance for discriminating lung cancer cases and controls.

Abstract: Diagnosis of lung cancer patients with indeterminate pulmonary nodules (IPNs) presents a significant clinical challenge, with morbidity and management costs of $28 billion/year. We show that a quantitative free-solution assay (FSA), coupled with a compensated interferometric reader (CIR) improves the diagnostic performance of CYFRA 21-1 as a lung cancer biomarker. FSA-CIR is a rapid, mix-and-read, isothermal, label- and enzyme-free, matrix-insensitive, target and probe-agnostic assay. Operating FSA-CIR at ~40, 0.75 μL samples/day delivered a serum CYFRA 21-1 limit of quantification (LOQ) of 81 pg/mL with intra-assay and inter-assay CVs of 4.9% and 9.6% for four-day replicate determinations. Blinded analysis of a 225 patient cohort, consisting of 75 nonmalignant nodules, 45 adenocarcinomas, 44 squamous cell carcinomas, and 61 small cell lung cancers, gave a clear separation of cases and controls, not observed in the Cobas ECL analysis. The area under the curve (AUC) for the Mayo model increased from 0.595 to 0.923 when combined with the FSA-CIR CYFRA 21-1 measurements. In a population with nodules between 6-30 mm, the AUC increased from 0.567 to 0.943. In this subgroup, the positive predictive value (PPV) for all tumors by the CYFRA 21-1 assay was 98.7%. Our results demonstrate increased performance of the CYFRA 21-1 assay using FSA-CIR and represents a proof of concept for redefining the performance characteristics of this important candidate biomarker.

Introduction

Lung cancer is the leading cause of cancer-related deaths in the United States (1). Low dose chest CT screening programs that target high-risk individuals can reduce the relative risk for lung cancer-specific mortality by 20% in the context of a randomized clinical trial (2). There is a growing movement to implement this life saving screening into clinical practice, with endorsements from the U.S. Preventive Services Task Force (3), the vast majority of professional societies (4), and a willingness from payers to provide reimbursement (3-4). Yet, numerous challenges still need to be navigated to provide improved outcomes. Among those are: a) how to position a biomarker prior to chest CT screening to decrease the cost and rates of false positive tests; b) how to address the diagnosis of lung cancer among indeterminate pulmonary nodules (IPNs); and c) how to detect recurrence. The availability of a rapid, high-sensitivity detection method to improve the quantification of biomarkers has the potential to expand individualized management of indeterminate pulmonary nodules (IPNs) in lung cancer patients.

Redefining the value of strong candidate biomarkers could produce changes in the guidelines for the management of IPNs, for disease monitoring, and for the early detection of cancer in the preclinical stage. Our approach addresses how current clinical blood biomarker strategies are too insensitive to enable detection of a developing tumor within the first decade of tumor growth (5) and mirrors what was accomplished when a *high sensitivity* version of the CRP assay was demonstrated. Because of improved sensitivity, the *h*-CRP test, performed widely today, allowed an otherwise nondiscriminatory biomarker to be repurposed, transforming it into a clinically useful target for determining initial status of a patient with a suspect cardiac event (6). Others have taken this tactic of addressing biomarker value by attempting to increase the sensitivity of the assay (7). While promising results have been obtained, until now there has been no definitive report showing significant improvement in positive predictive value (PPV) and diagnostic likelihood ratio (DLR) values for lung cancer from a single protein lung cancer biomarker.

Numerous biomarker approaches have been reported for the study of cancer pathogenesis, albeit clinical translation has been problematic. Among the most common assay methods are ELISA, electrochemiluminescence (ECL) (8), and bead array technologies (9). Label-free techniques, such as surface plasmon resonance (SPR) (10), quartz-crystal microbalance (11), wave-guided interferometry (12), and mass spectrometry (MS) have been employed for biomarker quantification, but have yet to provide an improvement in diagnostic power (13). Although MS has been exceedingly valuable in the biomarker discovery phase (14), instrumentation complexity and difficulty with quantification make its use for clinical screening unattractive (15). Multiplexed MRM/MS targeted assays using stable-isotope-labeled peptide standards for accurate quantitation are showing promise as clinical diagnostic assays (16), but complexity and low-throughput remain as limitations. There are now platforms available that are reported to have single-molecule sensitivity that have emerged. These techniques still employ a fluorescence sandwich assay based on multiple chemical steps. Singulex uses single molecule counting technology to obtain high sensitivity for biomarker targets (17) by using a microparticle to capture the target and a separation step to yield a bead with the fluorescently labeled target. Then, by limiting the probe volume to a few femtoliters, as in con-focal microscopy, low copy numbers are counted. Simoa (Single Molecule Array) from Quanterix is a technology that exploits the advantages of digital assays. Again a sandwich assay on beads is performed, but here each bead is collected in micro-wells formed at the end of a coherent fiber bundle or similar small volume receptacle (18). While

promising, both of these techniques have deficiencies, related to speed, reproducibility, cost, and/or accessibility. SOMALOGIC has taken a different approach to quantifying serum proteins by employing aptamers, which are stands of DNA or RNA selected to bind the target (19). Their detection approach capitalizes on a slow 'off-rate' for one of the complexes formed to separate the sample from background (20). While this aptamer-probe method has shown promise (21), multiple (as many as 10) sample handling and labeling steps, combined with relatively complicated instrumentation has impeded the wide dissemination of the technology for biomarker quantification.

In general, platforms that require either surface immobilization and/or labeling steps can make assay development and species validation arduous, slow, and expensive. Given these observations, we have chosen to explore the potential to do biomarker quantification label-free and in free-solution. The Free-Solution Assay (FSA) presented here appears to represent a viable alternative (22) to many of the existing and emerging assays. FSA is a mix-and-read approach that is assay agnostic, highly sensitive, rapid, and matrix independent. It will be shown here that when FSA is combined with a recently demonstrated compensated interferometric reader (CIR), it is possible to quantify the protein biomarker CYFRA 21-1 rapidly in serum samples at levels significantly lower than the gold standard approach (limits of quantitation (LOQ) 81 pg/mL vs. 500 pg/mL for ECL (23)).

We hypothesized that this lower limit of quantitation (LOQ) could transform biomarker utility, as with *h*-CRP, allowing improved detection for the early diagnosis of lung cancer in patients with indeterminate pulmonary nodules (IPNs). Resetting the detectable concentrations of one of the best candidate biomarkers for lung cancer, CYFRA 21-1 in serum, can thereby significantly improving its clinical utility by increasing the discriminatory power of the biomarker. CYFRA 21-1, a fragment of the protein cytokeratin-19, has been implicated in numerous tumors and suggested as potential biomarker candidates (24), and has a long history of being investigated as a potential lung cancer biomarker (25). Yet, to date, insufficient sensitivity and specificity has limited the value of CYFRA 21-1 in clinical practice. Even so, CYFRA 21-1 currently serves as a blood-based non-small cell lung cancer (NSCLC) biomarker with concentrations correlated to disease progression (26). As for its diagnostic utility in lung cancer, CYFRA 21-1 has been restricted by the constitutive expression of 2.4 ng/mL in healthy individuals (27), a value near the reported measurement range (or LOQ) for ELISA (1.0-2.95 ng/mL). Our preliminary observations with backscattering interferometry (BSI) showed that our FSA, based on a single antibody probe to CYFRA 21-1 and read by an interferometer, can provide up to 40-fold LOQ improvements for serum biomarker quantification, when compared to established enzyme-linked immunosorbent assays (ELISAs) (28). Here we build on these observations, reporting a new higher throughput interferometer, compensated for enhanced S/N performance and the application of our FSA to quantify CYFRA 21-1 in a clinically relevant patient population.

Results

1. FSA-CIR provides high sensitivity analysis of serum protein.

Several factors reported here, including the enhancement of detection sensitivity and specificity, are important in the lung cancer biomarker detection approach. The first is the compensated interferometer (29), which is based on a simple optical train that consists of a diode laser, an object (capillary tube), and a camera (**Fig. 1**). The compensation approach has enabled

the elimination of the high-resolution temperature controller, typically needed for such devices (30) and greatly simplifies the complexity of the device (**Fig. S1**).

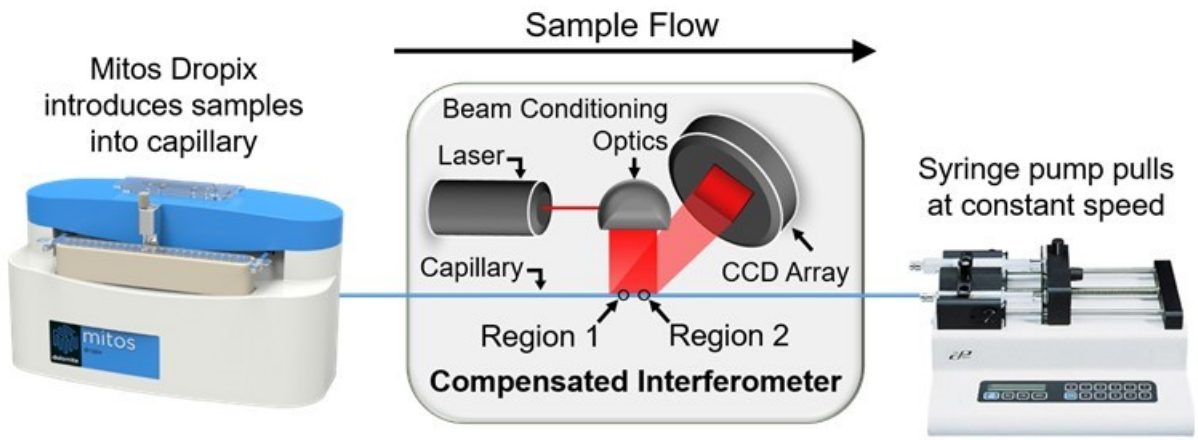

Fig. 1. Workflow of the compensated interferometric reader. Block diagram CIR, showing the Mitos Dropix droplet generator (left), laser and fringe detector (center), and syringe pump (right). Sample-Reference droplet pairs move through the detection region at constant flow rate and are measured in real time.

Second, marrying the interferometer with a slightly modified commercial droplet generator (Mitos Dropix, Dolomite Microfluidics, Royston, UK), and an inexpensive syringe pump results in a compensated interferometric reader (CIR) (**Fig. 1**). Modifications of the Dropix included retooling the sample collection hook to facilitate the use of a capillary tube and the development of multi-well biocompatible sample holders with low non-specific adsorption. CIR has significantly increased sample throughput, improved sensitivity, and constrains sample volume relative to previous interferometers (31).

Third, our compensation method eliminates the need to regulate temperature, allowing capillary cells to be used in our reader (32). Employing a fused silica capillary tube in CIR is advantageous, because it allows for seamless sample droplet train generation and it provides enhanced S/N over chip-based optical designs (33). The continuous transfer line approach provides for the production of smooth, uninterrupted sample droplet trains. Collectively, when compared to previous interferometric sensor designs (31), the CIR provides significantly increased throughput, streamlined data collection and analysis, and constrains sample size to less than 1 µL.

CIR enables trains of sample and reference solutions, separated by an oil droplet, to be interrogated by a single laser beam (**Fig. 1**). Simultaneous interrogation of the sample and reference solutions, by a single beam, provides compensation for laser pointing instability, wavelength wander, intensity fluctuations, and environmental temperature perturbations (29). In addition, comparison of composition-matched sample – reference pairs, allows matrix insensitive operation for biomarker quantification. The measurement results from the laser illuminating the capillary, the beam being reflected/refracted by the tube, producing a set of very high contrast, elongated, interference fringes (**Fig. S1**). When the composition (refractive index, RI) of the fluid in the detection window of the capillary changes, the fringes shift spatially. Comparison of these positional shifts in two adjacent regions/windows of the capillary yield a differential a measurement (29). These relative positional fringe shifts are quantified using a Fast Fourier Transform (FFT) (22). The FFT and an in-house image processing algorithm reports a phase

change difference for the sample and reference solutions, thereby enabling antibody-biomarker complex quantification.

Collectively, CIR provided probe-target binding assays with 81 pg/mL LOQs, at medium-throughput (40 sample/day), while constraining sample serum volumes to 0.75 µL. To our knowledge, CIR is the only nanoliter-volume interferometric reader based on an inexpensive diode laser, with this level of throughput and no need for a high resolution temperature controller (31).

2. The Free-solution Assay for CYFRA 21-1.

The free-solution assay (FSA) is also a key to the biomarker results presented here. The principal for FSA (22) is based on recording predictable and reproducible changes in the solution dipole moment from binding-induced changes in molecular conformation and hydration. In FSA, preparation and subtraction of index matched sample-reference pairs facilitates the elimination of matrix background. Using FSA with CIR affords the direct comparison of these sample pairs resulting in label-free, solution-phase target quantification in complex milieu, at sensitivities comparable, or better than many fluorescent assays (pg/mL) (28, 34). **Fig. 2** illustrates the workflow for FSA. First, a small volume of serum is split into two aliquots to provide 'test' and 'reference' solutions. Next, we add an excess of antibody probe to one of these aliquots, giving the test sample. Third, the "reference/control" is formed by adding an RI matching solution to the other aliquot. Both solutions are allowed to equilibrate for short period of time (~1 hr) and then introduced into adjacent wells of the droplet generator for analysis by the interferometer as pairs separated by an oil droplet.

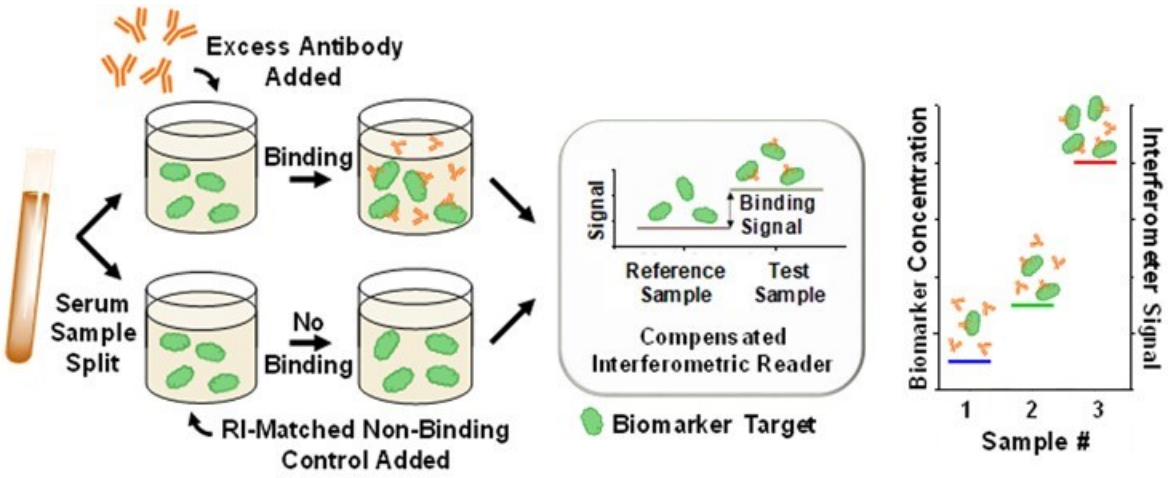

Fig. 2. Schematic of the Free-solution assay method. Samples are split into two aliquots. An excess of the probe antibody is introduced to the binding sample, while an RI-matched non-binding control solution is added to the reference sample. The CIR reports a signal that correlates with the resulting changes in conformation and hydration of the probe/target molecules upon binding.

To test our hypothesis that lowered LOQs for serum proteins can improve their clinical utility as lung cancer biomarkers, the analytical performance of FSA-CIR for quantifying CYFRA 21-1 was established. Working with spiked 25% serum and a commercial antibody probe to CYRFA 21.1, we obtained high quality calibration on two different instruments, over a several day period and by two independent users. **Fig. 3** presents the combined calibration results for these 4 independent serum CYFRA 21-1 assays (individual curves found in **Fig. S2**). The plot also shows the average of all CYFRA 21-1 calibration curves, black line, and the 95% confidence

interval, dashed line and grey zone. The analytical figures of merit for these assays had correlation coefficients of R^2 = 0.98-0.99, a dynamic operating range of ~3.5 decades, excellent reproducibility and an average LOQ of 81 pg/mL. The standard deviation for all calibrations place the error well within the 95% confidence interval. When analyzing 0.75 µL droplets in our reader we obtained intra-assay CVs for 7 replicate droplet measurements of 4.9% and an inter-assay CV of 9.6% for four-day replicate determinations. The LOQs for CYFRA-21-1 reported here are equivalent to those published recently (LOQ of 80 pg/mL) for a somewhat complicated, chemically intensive immunoassay (34), and ~6-fold better than the ~500 pg/mL LOQ for the gold-standard, Cobas electrochemiluminescence assay (ECL) (23, 35). Using FSA-CIR we were able to perform the complete analysis of ~50 patient serum sample-reference pairs per day, including calibrations, and full data workup.

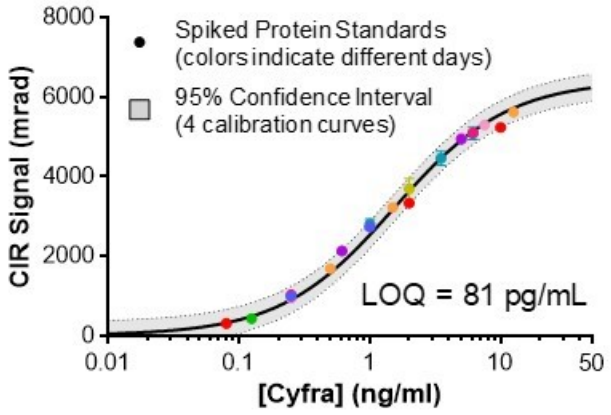

Fig. 3. The CYFRA 21-1 FSA calibration curve. The calibration curves for the CYFRA 21-1 FSA, with the spiked "unknowns" run across 4 calibrations plotted as the multicolored dots. Each color represents spiked unknowns that correlate to different calibrations. Error bars shown on plot.

As a test of assay accuracy, we prepared 'unknowns' by spiking serum with CYFRA 21-1 and blinding the sample identity to the instrument operator. **Fig. 3** presents the response for these spiked serum samples, with the error bars representing the standard deviation for 7 replicate determinations. **Table S2** shows that FSA-CIR provided a highly accurate result for these determinations, with the percent difference from the true CYFRA 21-1 concentrations ranging from 0.4% to 25%, except for one 10ng/mL 'unknown' which gave a 32% difference. It is noteworthy that this determination still fell within the 95% confidence interval (grey region, **Fig. 3**) and that the error would not impact case vs. control classification or the cut-off. Within the linear range of the calibration curve (0.08 to 4 ng/mL), FSA-CIR provided an average percent difference between actual and determined CYFRA 21-1 concentration of 10.9%.

3. Diagnostic performance testing in a case-control study of individuals presenting with lesions suspicious of lung cancer.

Using the mix-and-read assay and reader operating at 40 IPN serum samples/day, we performed a preliminary clinical test to address the two questions: 1) As with the high sensitivity-*CRP* assay (6a), can CYFRA 21-1 become a clinically useful by lowering the biomarker LOQ? 2) Can increasing biomarker assay sensitivity improve the diagnostic discriminatory power? To address these questions, we employed the calibration results presented above and analyzed 225 blinded serum samples of individuals presenting with lesions suspicious for lung cancer. These serum samples were collected prospectively following a standard operating procedure and were stored in our thoracic biorepository. The cohort consisted of 75 with nonmalignant nodules, 45 adenocarcinomas (stages 1 and 2), 44 squamous cell carcinomas (stages 1 and 2), and 61 small cell lung cancers (limited and extensive stages) (**Table 1**).

Fig. 4A illustrates (dashed lines), that the enhanced sensitivity of FSA-CIR for CYFRA 21-1 enabled the quantification of biomarker for all but several samples, whereas using the standard ELISA assay (LOQ of 1.2 ng/mL) it would have not been possible to accurately quantify the biomarker concentration in 98 of the 225 patient samples.

Table 1. Patient Characteristics.

	No Cancer	ADC	SCC	SCLC
	N=75	N=45	N=44	N=61
Age (Mean ± STDEV)	59.2 ± 12.7	65.2 ± 8.0	65.8 ± 7.8	63.9 ± 8.9
Gender (%)				
Male	40 (53)	26 (58)	29 (66)	36 (59)
Female	35 (47)	19 (42)	15 (34)	25 (41)
Smoking (%)				
Current	20 (27)	7 (16)	11 (25)	20 (33)
Ex	54 (72)	38 (84)	33 (75)	38 (62)
Never	1 (1)	0 (0)	0 (0)	3 (5)
Pack Years (Mean ± STDEV)	41.1 ± 30.3	50.1 ± 31.3	53.9 ± 23.5	63.7 ± 32.8
Nodule Size (cm) (Mean ± STDEV)	2.5 ± 1.6	2.7 ± 1.7	2.7 ± 2.0	3.6 ± 2.6
Path Staging (%)				
IA-IB	0 (0)	33 (73)	34 (77)	0 (0)
IIA-IIB	0 (0)	12 (27)	10 (23)	0 (0)
IIIA-IV	0 (0)	0 (0)	0 (0)	0 (0)
Limited	0 (0)	0 (0)	0 (0)	33 (54)
Extensive	0 (0)	0 (0)	0 (0)	28 (46)

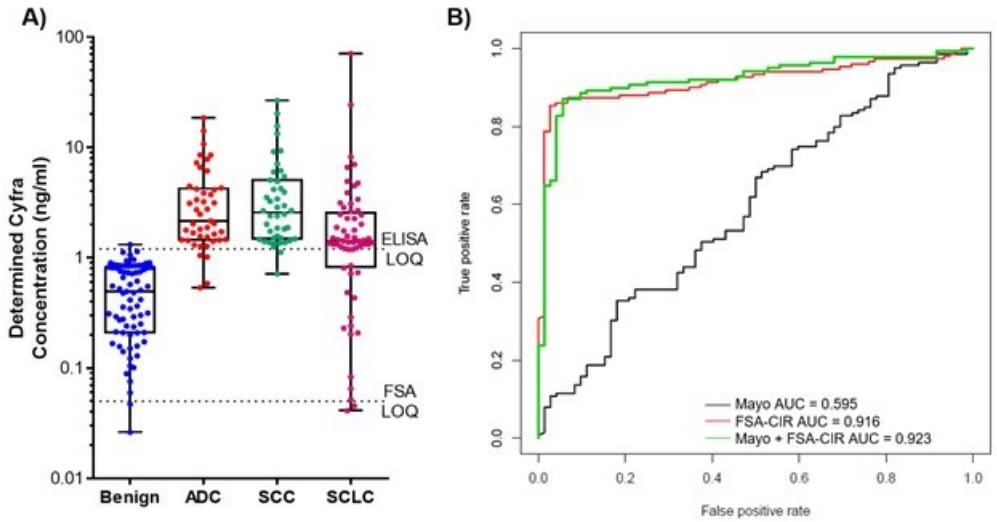

Fig. 4. Development of the CYFRA 21-1 FSA. A) Measurement of CYFRA 21-1 by FSA-CIR across individuals with benign lung nodules (Benign), Adenocarcinomas (ADCs), Stages 1 and 2 lung squamous cell carcinomas (SCCs), and all stage small cell lung cancers (SCLCs). **B)** ROC curve illustrating added value of FSA-CIR over clinical parameters and nodule size (the Mayo risk model) for the diagnosis of IPNs. N=225.

Using the Mayo model (36) for all patients presenting with IPNs, we tested our biomarker diagnostic performance against clinical predictors (37). Based on receiver operating characteristics (ROC) curve shown in **Fig. 4B**, our preliminary data suggest a strong benefit to the

FSA-CYFRA 21-1 assay for the Mayo model. The area under the curve (AUC) increases from 0.595 for the Mayo model to 0.923 when combining Mayo with CYFRA 21-1 measured by FSA-CIR. Further, the positive predictive value (PPV) for all tumors by the FSA-CYFRA 21-1 assay is 98.5% (**Table 2**).

Table 2. Diagnostic properties of CYFRA 21-1 by FSA-CIR.

	All Nodules	Nodules 6-30 mm
Sample Size	225	131
Sens	0.853	0.881
Spec	0.973	0.979
PPV	0.985	0.987
NPV	0.768	0.821
+DLR	32.00	41.40
-DLR	0.15	0.12
FP	2	1
FN	22	10

PPV, positive predictive value; NPV, negative predictive value; DLR, diagnostic likelihood ratio; FP, false positive; FN, false negative.

Next, we limited the analysis to individuals presenting with IPNs nodules between 6-30 mm in diameter. In this more clinically relevant patient population (38) the AUC for the Mayo model was 0.567, improving to 0.943 when combining Mayo with CYFRA 21-1 measured by FSA-CIR. Here the PPV by the FSA-CYFRA 21-1 is 99%. Further, with a positive diagnostic likelihood ratio of (+ DLR) of 41.4 and a negative (-DLR) of 0.12, the CYRFA 21-1 biomarker results indicate a potential for use in the early detection of lung cancer (including stage 1 disease).

4. Assay performance comparison.

An independent analysis was performed on aliquots of the same serum samples by a CLIA Lab at the University of Maryland, using the electrochemiluminescence immunoassay on the ElecSys 2010 system (Roche Diagnostics Corp., Indianapolis, IN). This immunoassay uses two specific monoclonal antibodies to form a sandwich, with the detection antibody labeled with a Ruthenium complex. When electric potential is applied to the sample in the Corbas reader, the captured complex emits light detected by a photomultiplier. The assay is reported to have a low coefficient of variation (2–5%) and an LOQ of 500pg/mL. The results of both ECL and FSA determinations are displayed in a box plot in **Fig. 5**. The figure shows that for this patient cohort, FSA-CIR analysis gave a clear separation of cases and controls that the ECL assay was unable to provide.

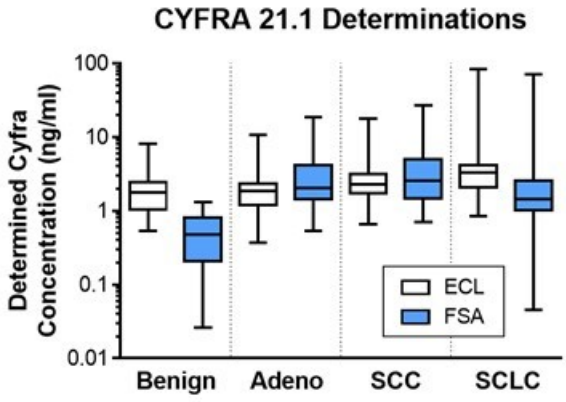

Fig. 5. Comparison between FSA and ECL CYFRA 21-1 measurements. Box plots illustrate CYFRA 21-1 by FSA and ECL across individuals with benign lung nodules (Benign), Adenocarcinomas (ADCs), Stages 1 and 2 lung squamous cell carcinomas (SCCs), and all stage small cell lung cancers (SCLCs).

5. Assay Robustness.

A preliminary evaluation of assay robustness was performed by repeating the serum CYFRA 21-1 measurements on 20 patient samples on subsequent days, and after additional freeze-thaw cycles. Test samples consisted of 10 controls, 5 adenocarcinomas, 5 squamous cell

carcinomas randomly selected by the clinic and blinded to the FSA-CIR operator. **Fig. 6** illustrates the results of this experiment, showing that the FSA-CIR method is relatively robust and repeatable over 3 days and 2 additional freeze-thaw cycles. The average three day CV for all sample determinations was 21.1%. Just one sample needed to be reclassified, likely due to mishandling of the sample during assay preparation, which currently requires several manual pipetting steps that are known to contribute to assay error (data not shown). An auto-pipetting device, as planned in the next generation instrument, should address this shortcoming. While more extensive testing of sample handling is necessary before formal translation to the clinic, the fact that we observed relatively small changes in the patient CYFRA 21-1 concentrations for these 20-blinded patient samples bodes well for use of the assay. At a minimum, the results indicate that a 3-day handling period and three freeze-thaw cycles can be tolerated.

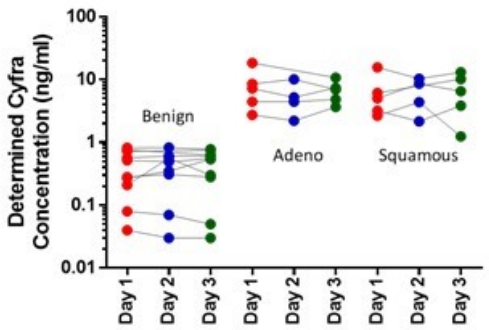

Fig. 6. Robustness of the CYFRA 21-1 FSA. A 20-patient subset (10 benign nodules, 5 adeno, 5 squamous) was subjected to repeated measurements on 2 subsequent days, with an additional freeze-thaw cycle before each measurement.

Discussion

In this report, it has been shown that combining a new interferometer with a droplet generator and a syringe pump results in a relatively simple microfluidic reader, the CIR. When combining this reader with FSA, a label-free, solution-phase assay, the result is a potentially revolutionary platform for biomarker validation and quantification because: 1) It's rapid, cost effective and label-free (no fluorescence or radiolabeling) measurement of unaltered or minimally processed patient samples; 2) Analysis can be effectively performed on <1 μL sample aliquots, allowing multiple replicates to be performed on quantity-limited samples; 3) The adjacent sample – reference droplet configuration allows for matrix insensitive operation and assay specificity; 4) Sensitivity of the FSA-CIR exceeds that of many, more complicated competing technologies. For example, when applied to clinically relevant samples, the FSA CYFRA 21-1 assay was shown to be at least 6-fold more sensitive than the more complicated ECL method. 5) The optical engine of CIR is simple, consisting of a diode laser, capillary tube, and camera. This simplicity, combined with the elimination of a high-resolution temperature controller, opens the avenue to construct a benchtop or battery-operated hand-held reader.

FSA represents a unique approach to biomarker quantification, operating as a mix-and-read, label-free, solution-phase approach, based on transducing binding induced polarizability changes (RI) resulting from conformation and hydration changes. We anticipate the ability to rapidly screen additional potential serum biomarkers with numerous probe variations (antibodies, DNA/RNA aptamers, and small molecules) (39), could help reduce the biomarker validation bottleneck and aid in expediting clinical translation.

Lung cancer continues to be one the most difficult diseases to diagnose early, and non-invasively, yet reports suggest that screening (2) does represents an opportunity impact diagnosis of early stage disease. In the near term, challenges to early detection include: a) how to discriminate benign from malignant disease among people presenting with IPNs; and b) how to position biomarker use prior to chest CT screening to eventually detect preclinical disease. Here

we tested a hypothesis that, by virtue of lower LOQs afforded by FSA-CIR CYFRA-21.1 measurements, it would possible to improve diagnostic performance. This approach works by redefining the concentration of the candidate biomarker (CYFRA 21-1) in the control population. This population includes IPNs with no evidence of growth at 2 years of follow up and therefore considered benign.

In a 225-patient cohort, a >6-fold better serum biomarker LOQ led to a significantly improved clinical performance for CYFRA 21-1. Here we demonstrated that lowering the LOQ for CYFRA 21-1 increases the area under the curve (AUC), based on the Mayo model, from 0.595 to 0.923. Employing a single monoclonal antibody assay approach enabled a +DLR of 32 and a PPV of 98.5% using a cutoff of 1.19 ng/mL in a 225-patient case-control study. To our knowledge this is first report where a single biomarker of lung cancer exhibited performance metrics of 85% sensitivity and 97% specificity in a patient cohort of IPNs (27, 40). With our method, additional individuals can be classified (indeterminate or not) as a result of obtaining a true biomarker concentration, where it had not been possible with less sensitive assays. ECL Cobas assay was performed on the patient cohort in a CLIA laboratory as an independent validation of our observations with CYFRA 21-1. In this head-to-head comparison our assay methodology provided a measurable case and control separation, not provided by the ECL. The improvements in biomarker predictive capability illustrated here are among the best reported, particularly for a single biomarker. Ultimately, we envision integrating our method with clinical and imaging data to potentially further improve managing this difficult patient population.

While a more stringent clinical validation is needed, our results suggest it may be possible to address a major hurdle in the management of patients with IPNs / lung cancer by implementing a higher sensitivity biomarker assay into the clinical setting.

Acknowledgments: Funding: Part of this study was funded by CA186145 and CA152662 awarded to P.P.M., as well as NSF CHE 1610964 to D.J.B. Roche is recognized for partial funding for the ECL assay or for the contribution of the ELC assay chemistry. **Author contributions**: D.J.B. and P.P.M. designed research. M.N.K., A.K.K., and D.J.B. contributed to instrument design and FSA development. M.N.K, R.L.W. and A.K.K. collected FSA data. M.N.K., A.K.K., and D.J.B. analyzed FSA data. R.C. performed ECL analysis. M.H. compiled the patient cohort, samples, and clinical information. H.C. performed biostatistics analysis. T.M. and M.P. performed independent biostatics analysis. D.J.B. and P.P.M., with input from the entire team. **Competing interests**: D.J.B. is inventor on issued patent US 9,638,632 B2, which covers a multiplexed interferometric detection system. D.J.B. and M.N.K. are inventors on submitted patent application US2016/0327480 which covers the compensated interferometer. D.J.B., M.N.K., and A.K.K. are inventors on submitted patent application WO2017/132483, which covers methods for the measurement of molecular interactions by refractive index sensing. All other authors declare no competing interest. **Data and materials availability**: All reagents needed to run assays can be purchased or prepared as described. All components required to build the compensated interferometer can be purchased and fabricated as defined here. Raw data and the data collection and analysis Labview code for CIR are both available upon request.

Supplementary Materials

Fig. S1. Block Diagram of the Compensated Interferometer.

Fig. S2. Four replicate FSA-CIR calibration curves using spiked protein standards.

Table S1. Analytical figures of merit for four replicate FSA-CIR calibration curves.

Table S2. Phantom "Unknowns." Values in ng/mL.

References and Notes:

1. Siegel, R. L.; Miller, K. D.; Jemal, A., Cancer Statistics, 2015. *Ca-Cancer J Clin* **2015,** *65* (1), 5-29.
2. Aberle, D. R.; Adams, A. M.; Berg, C. D.; Black, W. C.; Clapp, J. D.; Fagerstrom, R. M.; Gareen, I. F.; Gatsonis, C.; Marcus, P. M.; Sicks, J. D., Reduced Lung-Cancer Mortality with Low-Dose Computed Tomographic Screening. *New Engl J Med* **2011,** *365* (5), 395-409.
3. Moyer, V. A.; Force, U. S. P. S. T., Screening for lung cancer: U.S. Preventive Services Task Force recommendation statement. *Ann Intern Med* **2014,** *160* (5), 330-338.
4. Wiener, R. S.; Gould, M. K.; Arenberg, D. A.; Au, D. H.; Fennig, K.; Lamb, C. R.; Mazzone, P. J.; Midthun, D. E.; Napoli, M.; Ost, D. E.; Powell, C. A.; Rivera, M. P.; Slatore, C. G.; Tanner, N. T.; Vachani, A.; Wisnivesky, J. P.; Yoon, S. H.; Lung, A. C. C. L.-D. C., An Official American Thoracic Society/American College of Chest Physicians Policy Statement: Implementation of Low-Dose Computed Tomography Lung Cancer Screening Programs in Clinical Practice. *American Journal of Respiratory and Critical Care Medicine* **2015,** *192* (7), 881-891.
5. Hori, S. S.; Gambhir, S. S., Mathematical model identifies blood biomarker-based early cancer detection strategies and limitations. *Sci Transl Med* **2011,** *3* (109), 109ra116.
6. (a) Rifai, N.; Ridker, P. M., High-sensitivity C-reactive protein: a novel and promising marker of coronary heart disease. *Clin Chem* **2001,** *47* (3), 403-11; (b) Ridker, P. M.; Rifai, N.; Clearfield, M.; Downs, J. R.; Weis, S. E.; Miles, J. S.; Gotto, A. M., Jr.; Air Force/Texas Coronary Atherosclerosis Prevention Study, I., Measurement of C-reactive protein for the targeting of statin therapy in the primary prevention of acute coronary events. *The New England journal of medicine* **2001,** *344* (26), 1959-65; (c) Chaturvedi, A. K.; Caporaso, N. E.; Katki, H. A.; Wong, H. L.; Chatterjee, N.; Pine, S. R.; Chanock, S. J.; Goedert, J. J.; Engels, E. A., C-reactive protein and risk of lung cancer. *Journal of clinical oncology : official journal of the American Society of Clinical Oncology* **2010,** *28* (16), 2719-26.
7. (a) Chen, Z. H.; Liang, R. L.; Guo, X. X.; Liang, J. Y.; Deng, Q. T.; Li, M.; An, T. X.; Liu, T. C.; Wu, Y. S., Simultaneous quantitation of cytokeratin-19 fragment and carcinoembryonic antigen in human serum via quantum dot-doped nanoparticles. *Biosens Bioelectron* **2017,** *91*, 60-65; (b) Li, J.; Skeete, Z.; Shan, S. Y.; Yan, S.; Kurzatkowska, K.; Zhao, W.; Ngo, Q. M.; Holubovska, P.; Luo, J.; Hepel, M.; Zhong, C. J., Surface Enhanced Raman Scattering Detection of Cancer Biomarkers with Bifunctional Nanocomposite Probes. *Analytical chemistry* **2015,** *87* (21), 10698-10702.
8. (a) Wang, J.; Ahmad, H.; Ma, C.; Shi, Q. H.; Vermesh, O.; Vermesh, U.; Heath, J., A self-powered, one-step chip for rapid, quantitative and multiplexed detection of proteins from pinpricks of whole blood. *Lab Chip* **2010,** *10* (22), 3157-3162; (b) Fan, R.; Vermesh, O.; Srivastava, A.; Yen, B. K. H.; Qin, L. D.; Ahmad, H.; Kwong, G. A.; Liu, C. C.; Gould, J.; Hood, L.; Heath, J. R., Integrated barcode chips for rapid, multiplexed analysis of proteins in microliter quantities of blood. *Nature biotechnology* **2008,** *26* (12), 1373-1378; (c) Garcia-Cordero, J. L.; Maerkl, S. J., A 1024-sample serum analyzer chip for cancer diagnostics. *Lab Chip* **2014**, DOI: 10.1039/c3lc51153g.
9. Lee, H. J.; Kim, Y. T.; Park, P. J.; Shin, Y. S.; Kang, K. N.; Kim, Y.; Kim, C. W., A novel detection method of non–small cell lung cancer using multiplexed bead-based serum biomarker profiling. *The Journal of Thoracic and Cardiovascular Surgery* **2012,** *143* (2), 421-427.e3.
10. (a) Lee, H. J.; Nedelkov, D.; Corn, R. M., Surface plasmon resonance imaging measurements of antibody arrays for the multiplexed detection of low molecular weight protein biomarkers. *Analytical chemistry* **2006,** *78* (18), 6504-6510; (b) Teramura, Y.; Iwata, H., Label-free immunosensing for alpha-fetoprotein in human plasma using surface plasmon resonance. *Analytical biochemistry* **2007,** *365* (2), 201-207.

11. Huang, C. S.; Chaudhery, V.; Pokhriyal, A.; George, S.; Polans, J.; Lu, M.; Tan, R. M.; Zangar, R. C.; Cunningham, B. T., Multiplexed Cancer Biomarker Detection Using Quartz-Based Photonic Crystal Surfaces. *Analytical chemistry* **2012,** *84* (2), 1126-1133.
12. (a) Cunningham, B.; Li, P.; Lin, B.; Pepper, J., Colorimetric resonant reflection as a direct biochemical assay technique. *Sensor Actuat B-Chem* **2002,** *81* (2-3), 316-328; (b) Cunningham, B. T.; Laing, L., Microplate-based, label-free detection of biomolecular interactions: applications in proteomics. *Expert Rev Proteomics* **2006,** *3* (3), 271-81.
13. Guerra, E. N. S.; Rêgo, D. F.; Elias, S. T.; Coletta, R. D.; Mezzomo, L. A. M.; Gozal, D.; De Luca Canto, G., Diagnostic accuracy of serum biomarkers for head and neck cancer: A systematic review and meta-analysis. *Critical Reviews in Oncology / Hematology* **2016,** *101*, 93-118.
14. Mischak, H.; Schanstra, J. P., CE-MS in biomarker discovery, validation, and clinical application. *Proteom Clin Appl* **2011,** *5* (1-2), 9-23.
15. Diamandis, E. P., Biomarker validation is still the bottleneck in biomarker research. *Journal of internal medicine* **2012,** *272* (6), 620-620.
16. Gillette, M. A.; Carr, S. A., METHOD OF THE YEAR Quantitative analysis of peptides and proteins in biomedicine by targeted mass spectrometry. *Nat Methods* **2013,** *10* (1), 28-34.
17. Gilbert, M.; Livingston, R.; Felberg, J.; Bishop, J. J., Multiplex single molecule counting technology used to generate interleukin 4, interleukin 6, and interleukin 10 reference limits. *Analytical biochemistry* **2016,** *503*, 11-20.
18. (a) Rissin, D. M.; Kan, C. W.; Campbell, T. G.; Howes, S. C.; Fournier, D. R.; Song, L.; Piech, T.; Patel, P. P.; Chang, L.; Rivnak, A. J.; Ferrell, E. P.; Randall, J. D.; Provuncher, G. K.; Walt, D. R.; Duffy, D. C., Single-molecule enzyme-linked immunosorbent assay detects serum proteins at subfemtomolar concentrations. *Nature biotechnology* **2010,** *28* (6), 595-599; (b) Rissin, D. M.; Kan, C. W.; Song, L. N.; Rivnak, A. J.; Fishburn, M. W.; Shao, Q. C.; Piech, T.; Ferrell, E. P.; Meyer, R. E.; Campbell, T. G.; Fournier, D. R.; Duffy, D. C., Multiplexed single molecule immunoassays. *Lab Chip* **2013,** *13* (15), 2902-2911.
19. Gold, L.; Ayers, D.; Bertino, J.; Bock, C.; Bock, A.; Brody, E. N.; Carter, J.; Dalby, A. B.; Eaton, B. E.; Fitzwater, T.; Flather, D.; Forbes, A.; Foreman, T.; Fowler, C.; Gawande, B.; Goss, M.; Gunn, M.; Gupta, S.; Halladay, D.; Heil, J.; Heilig, J.; Hicke, B.; Husar, G.; Janjic, J.; Jarvis, T.; Jennings, S.; Katilius, E.; Keeney, T. R.; Kim, N.; Koch, T. H.; Kraemer, S.; Kroiss, L.; Le, N.; Levine, D.; Lindsey, W.; Lollo, B.; Mayfield, W.; Mehan, M.; Mehler, R.; Nelson, S. K.; Nelson, M.; Nieuwlandt, D.; Nikrad, M.; Ochsner, U.; Ostroff, R. M.; Otis, M.; Parker, T.; Pietrasiewicz, S.; Resnicow, D. I.; Rohloff, J.; Sanders, G.; Sattin, S.; Schneider, D.; Singer, B.; Stanton, M.; Sterkel, A.; Stewart, A.; Stratford, S.; Vaught, J. D.; Vrkljan, M.; Walker, J. J.; Watrobka, M.; Waugh, S.; Weiss, A.; Wilcox, S. K.; Wolfson, A.; Wolk, S. K.; Zhang, C.; Zichi, D., Aptamer-Based Multiplexed Proteomic Technology for Biomarker Discovery. *PloS one* **2010,** *5* (12), e15004.
20. Russell, T. M.; Green, L. S.; Rice, T.; Kruh-Garcia, N. A.; Dobos, K.; De Groote, M. A.; Hraha, T.; Sterling, D. G.; Janjic, N.; Ochsner, U. A., Potential of High-Affinity, Slow Off-Rate Modified Aptamer Reagents for Mycobacterium tuberculosis Proteins as Tools for Infection Models and Diagnostic Applications. *J Clin Microbiol* **2017,** *55* (10), 3072-3088.
21. Chen, C.; Zhou, S.; Cai, Y.; Tang, F., Nucleic acid aptamer application in diagnosis and therapy of colorectal cancer based on cell-SELEX technology. *npj Precision Oncology* **2017,** *1* (1), 37.
22. Bornhop, D. J.; Kammer, M. N.; Kussrow, A.; Flowers, R. A., 2nd; Meiler, J., Origin and prediction of free-solution interaction studies performed label-free. *Proc Natl Acad Sci USA* **2016,** *113* (12), E1595-604.
23. Diagnostics, R. Elecsys CYFRA 21-1. https://usdiagnostics.roche.com/products/11820966160/PARAM236/overlay.html.
24. Barak, V.; Goike, H.; Panaretakis, K. W.; Einarsson, R., Clinical utility of cytokeratins as tumor markers. *Clin Biochem* **2004,** *37* (7), 529-540.
25. (a) Takada, M.; Masuda, N.; Matsuura, E.; Kusunoki, Y.; Matui, K.; Nakagawa, K.; Yana, T.; Tuyuguchi, I.; Oohata, I.; Fukuoka, M., Measurement of cytokeratin 19 fragments as a marker of lung cancer by CYFRA 21-1 enzyme immunoassay. *British Journal Of Cancer* **1995,** *71*, 160; (b) Pastor, A.; Menendez, R.; Cremades, M.; Pastor, V.; Llopis, R.; Aznar, J., Diagnostic value of SCC, CEA and CYFRA 21.1 in lung cancer: a Bayesian analysis. *European Respiratory Journal* **1997,** *10* (3), 603-609.
26. (a) Molina, R.; Filella, X.; Augé, J. M.; Fuentes, R.; Bover, I.; Rifa, J.; Moreno, V.; Canals, E.; Viñolas, N.; Marquez, A.; Barreiro, E.; Borras, J.; Viladiu, P., Tumor Markers (CEA, CA 125, CYFRA 21-1, SCC and NSE) in Patients with Non-Small Cell Lung Cancer as an Aid in Histological Diagnosis and Prognosis. *Tumor Biology* **2003,** *24* (4), 209-218; (b) Molina, R.; Marrades, R. M.; Augé, J. M.; Escudero, J. M.; Viñolas, N.; Reguart, N.; Ramirez, J.; Filella, X.; Molins, L.; Agustí, A., Assessment of a Combined Panel of Six Serum Tumor Markers for Lung

Cancer. *American Journal of Respiratory and Critical Care Medicine* **2016,** *193* (4), 427-437; (c) Integrative Analysis of Lung Cancer, E.; Risk Consortium for Early Detection of Lung, C., Assessment of lung cancer risk on the basis of a biomarker panel of circulating proteins. *JAMA Oncology* **2018**, e182078.
27. (a) Rastel, D.; Ramaioli, A.; Cornillie, F.; Thirion, B., CYFRA 21-1, a sensitive and specific new tumour marker for squamous cell lung cancer. Report of the first European multicentre evaluation. CYFRA 21-1 Multicentre Study Group. *European journal of cancer* **1994,** *30A* (5), 601-6; (b) Karnak, D.; Ulubay, G.; Kayacan, O.; Beder, S.; Ibis, E.; Oflaz, G., Evaluation of Cyfra 21-1: a potential tumor marker for non-small cell lung carcinomas. *Lung* **2001,** *179* (1), 57-65; (c) Wieskopf, B.; Demangeat, C.; Purohit, A.; Stenger, R.; Gries, P.; Kreisman, H.; Quoix, E., Cyfra 21-1 as a biologic marker of non-small cell lung cancer. Evaluation of sensitivity, specificity, and prognostic role. *Chest* **1995,** *108* (1), 163-9.
28. Olmsted, I. R.; Hassanein, M.; Kussrow, A.; Hoeksema, M.; Li, M.; Massion, P. P.; Bornhop, D. J., Toward rapid, high-sensitivity, volume-constrained biomarker quantification and validation using backscattering interferometry. *Analytical chemistry* **2014,** *86* (15), 7566-74.
29. Kammer, M. N.; Kussrow, A. K.; Olmsted, I. R.; Bornhop, D. J., A Highly Compensated Interferometer for Biochemical Analysis. *ACS sensors* **2018,** *3* (8), 1546-1552.
30. Kammer, M. N.; Kussrow, A. K.; Bornhop, D. J., Longitudinal pixel averaging for improved compensation in backscattering interferometry. *Optics letters* **2018,** *43* (3), 482-485.
31. Kussrow, A.; Enders, C. S.; Bornhop, D. J., Interferometric Methods for Label-Free Molecular Interaction Studies. *Analytical chemistry* **2012,** *84* (2), 779-792.
32. Zhang, X. P.; Peng, W.; Zhang, Y., Fiber Fabry-Perot interferometer with controllable temperature sensitivity. *Optics letters* **2015,** *40* (23), 5658-5661.
33. (a) Swinney, K.; Markov, D.; Bornhop, D. J., Chip-scale universal detection based on backscatter interferometry. *Analytical chemistry* **2000,** *72* (13), 2690-2695; (b) Tarigan, H. J.; Neill, P.; Kenmore, C. K.; Bornhop, D. J., Capillary-scale refractive index detection by interferometric backscatter. *Analytical chemistry* **1996,** *68* (10), 1762-1770; (c) Schmitt, K.; Schirmer, B.; Hoffmann, C.; Brandenburg, A.; Meyrueis, P., Interferometric biosensor based on planar optical waveguide sensor chips for label-free detection of surface bound bioreactions. *Biosens Bioelectron* **2007,** *22* (11), 2591-7.
34. He, A.; Liu, T. C.; Dong, Z. N.; Ren, Z. Q.; Hou, J. Y.; Li, M.; Wu, Y. S., A novel immunoassay for the quantization of CYFRA 21-1 in human serum. *Journal of clinical laboratory analysis* **2013,** *27* (4), 277-83.
35. Muzyka, K., Current trends in the development of the electrochemiluminescent immunosensors. *Biosens Bioelectron* **2014,** *54*, 393-407.
36. Swensen, S. J.; Silverstein, M. D.; Ilstrup, D. M.; Schleck, C. D.; Edell, E. S., The probability of malignancy in solitary pulmonary nodules - Application to small radiologically indeterminate nodules. *Arch Intern Med* **1997,** *157* (8), 849-855.
37. Atwater, T.; Cook, C. M.; Massion, P. P., The Pursuit of Noninvasive Diagnosis of Lung Cancer. *Semin Resp Crit Care* **2016,** *37* (5), 670-680.
38. Deppen, S. A.; Grogan, E. L., Using Clinical Risk Models for Lung Nodule Classification. *Semin Thorac Cardiov* **2015,** *27* (1), 30-35.
39. Kammer, M. N.; Olmsted, I. R.; Kussrow, A. K.; Morris, M. J.; Jackson, G. W.; Bornhop, D. J., Characterizing aptamer small molecule interactions with backscattering interferometry. *The Analyst* **2014,** *139* (22), 5879-84.
40. (a) Guergova-Kuras, M.; Kurucz, I.; Hempel, W.; Tardieu, N.; Kadas, J.; Malderez-Bloes, C.; Jullien, A.; Kieffer, Y.; Hincapie, M.; Guttman, A.; Csanky, E.; Dezso, B.; Karger, B. L.; Takacs, L., Discovery of Lung Cancer Biomarkers by Profiling the Plasma Proteome with Monoclonal Antibody Libraries. *Molecular & Cellular Proteomics* **2011,** *10* (12), M111.010298; (b) Stieber, P.; Hasholzner, U.; Bodenmuller, H.; Nagel, D.; Sunderplassmann, L.; Dienemann, H.; Meier, W.; Fatehmoghadam, A., Cyfra 21-1 - a New Marker in Lung-Cancer. *Cancer* **1993,** *72* (3), 707-713.